

# Smart composites with controlled anisotropy

Zsolt Varga, Genovéva Filipcsei, Miklós Zrínyi\*

*HAS-BUTE Laboratory of Soft Matters, Department of Physical Chemistry, Budapest University of Technology and Economics, H-1521 Budapest, Hungary*

Received 21 July 2004; received in revised form 16 February 2005; accepted 15 March 2005

Available online 16 June 2005

## Abstract

The new generation of magnetic elastomers represents a new type of composites, consisting of small (mainly nano- and micron-sized) magnetic particles dispersed in a high elastic polymeric matrix. The combination of polymers with magnetic materials displays novel and often enhanced properties. The magnetic particles couple the shape of the elastomer to the external magnetic field. All of the forces acting on the particles are transmitted directly to the polymer chains resulting in either locomotion or deformation. Shape distortion occurs instantaneously and disappears abruptly when external field is applied or removed, respectively. Combination of magnetic and elastic properties leads to a number of striking phenomena that are exhibited in response to impressed magnetic field. Giant deformational effect, tuneable elastic modulus, non-homogeneous deformation and quick response to magnetic field open new opportunities for using such materials for various applications. Elastic materials with tailor-made anisotropy can also be prepared under external field. The anisotropy manifests itself in both direction dependent elastic modulus as well as direction dependent swelling.

© 2005 Elsevier Ltd. All rights reserved.

*Keywords:* Anisotropic magnetic elastomers; Stress induced softening; Einstein–Smallwood parameter

## 1. Introduction

Many useful engineering materials, as well as living organisms have a heterogeneous composition. The components of composite materials often have contradictory, but complementary properties. Fillers are usually solid additives that are incorporated into the polymer to modify the physical properties. Fillers can be divided into three categories: those that reinforce the polymer and improve its mechanical performance, those that are used to take up space, and thus reduce material costs. The third, less common, category is when filler particles are incorporated into the material to improve its responsive properties. Smart soft composites are valuable materials for several technological applications, e.g. vibration control.

Composite materials consisting of rather rigid polymeric matrices filled with magnetic particles have been known for a long time and are called magnetic elastomers. These materials are successfully used as permanent magnets, magnetic cores, connecting and fixing elements in many

areas. These traditional magnetic elastomers have low flexibility and practically do not change their size, shape and elastic properties in the presence of external magnetic field.

The new generation of magnetic elastomers represents a new type of composite, consisting of small (mainly nano- and micron-sized) magnetic particles dispersed in a highly elastic polymeric matrix [1–17]. The combination of polymers with magnetic materials displays novel and often enhanced properties. The magnetic particles couple the shape of the elastomer to the external magnetic field. All the forces acting on the particles are transmitted directly to the polymer chains, resulting in either locomotion or deformation. Shape distortion occurs instantaneously and disappears abruptly when external field is applied or removed, respectively. Combining magnetic and elastic properties leads to a number of striking phenomena that are exhibited in response to impressed magnetic field. Giant deformational effect, tuneable elastic modulus, non-homogeneous deformation and quick response to magnetic field open new opportunities for using such materials for various applications.

Elastic materials with tailor-made anisotropy can also be prepared under an external field. The anisotropy manifests itself both as a directionally dependent elastic modulus as well as in directionally dependent swelling. In this paper we

\* Corresponding author. Tel.: +36 1 463 3229; fax: +36 1 463 3767.  
E-mail address: [zrinyi@mail.bme.hu](mailto:zrinyi@mail.bme.hu) (M. Zrínyi).

report the preparation and mechanical properties of anisotropic composite elastomers. Two kinds of samples have been studied. Magnetic hydrogels made of chemically cross-linked poly(vinylalcohol) network filled with magnetite ( $\text{Fe}_3\text{O}_4$ ) as well as poly(dimethyl siloxane) elastomers loaded with carbonyl iron (Fe). The strength of interactions between the poly(vinylalcohol) chains and surface of magnetite is rather strong, whereas the chains of poly(dimethyl siloxane) adsorbs weakly onto the surface of iron and iron-oxide particles as well. The average size of the magnetic filler particles was varied from 4 nm to 1  $\mu\text{m}$ .

### 1.1. Magnetic gels and elastomers

A magnetic field sensitive gels and elastomers (abbreviated as magnetoelasts) are special type of filler-loaded polymer networks, where the finely divided filler particles have strong magnetic properties. Preparation of a magnetoelast does not require a special polymer or a special type of magnetic particle. As a polymer network one may use any flexible macromolecule that can be cross-linked. The filler particles can be obtained from ferri- and ferromagnetic materials. A highly responsive magnetoelast should have low elastic modulus and high initial susceptibility as well as high saturation magnetisation. The solid particles are the elementary carriers of a magnetic moment. In the absence of an applied field the magnetic moments are randomly oriented, and thus the polymer network has no net magnetization. If a magnetoelast is exposed to an external field, two distinct types of interactions can be identified: field–particle interaction, as well as particle–particle interaction [18]. If the field is non-uniform, then the field–particle interactions are dominant. Particles experience a magnetophoretic (MAP) force, respectively. As a result the particles are attracted to regions of stronger field intensities. Because of the cross-linking bridges in the network, changes in molecular conformation due to MAP forces can accumulate and lead to macroscopic shape changes as shown in Fig. 1. More information on magnetoelastic behaviour can be found in our previous papers [1–5,8,13].

In uniform field there are no attractive or repulsive field–particle interactions, therefore, particle–particle interactions

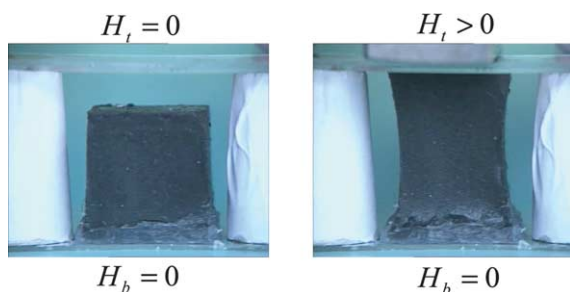


Fig. 1. Non-contact mode of elongation of a magnetite loaded PDMS network due to non-uniform magnetic field  $H_t$  and  $H_b$  represents the field intensity below ( $H_b$ ) and above ( $H_t$ ) the magnetoelast.

become dominant. In polymer solution the imposed field orients the magnetic dipoles. If the particles are spaced closely enough, such that their field can reach their neighbours a mutual particle interactions occur. This mutual interaction can be very strong, leading to significant change in the structure of particle ensembles. The particles attract each other when aligned end to end, and repel each other in side-by-side situation. Due to the attractive forces pearl chain structure develops as shown in Fig. 2.

### 1.2. Preparation of magnetic elastomers with homogeneous filler distribution

#### 1.2.1. Poly(dimethyl siloxane) (PDMS) networks

In order to prepare magnetic field responsive PDMS composites iron and  $\text{Fe}_3\text{O}_4$  particles were used as magnetic fillers. The concentration of the solid particles was varied between 10 and 30 wt% in the polymer matrix. Fig. 3 shows the scanning electron microscope (SEM) picture of the iron (Fig. 3(a)) and  $\text{Fe}_3\text{O}_4$  (Fig. 3(b)) particles.

It can be seen on the figures that polydisperse carbonyl iron particles have spherical shape with rather smooth surface. This is not the case for  $\text{Fe}_3\text{O}_4$  particles, they have smaller average size and narrower size distribution.

We have prepared iron and iron oxide ( $\text{Fe}_3\text{O}_4$ ) loaded poly(dimethyl siloxane) elastomers. The concentration of the filler particles in the elastomer was varied from 10 to 40 wt%.

PDMS networks were prepared from a commercial product of a two component reagent (Elastosil 604 A and Elastosil 604 B) provided by Wacker Co. These chemicals were used without further purification. Component A contains the monomers and the catalyst with Pt content while component B provides the cross-linking agent. Component B was varied from 2.45 to 3.48 wt%. The magnetite particles were dispersed in the Elastosil 604 A. After mixing it with the Elastosil 604 B component, the solution was transferred into a cube-shaped mould. To determine the gelation time, oscillation rheological measurements were performed. The measurement was carried out in HAAKE Rheostress RS 100 rheometer in oscillation mode using parallel plate geometry with 35 mm

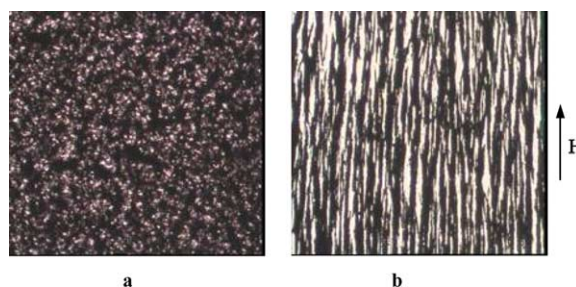
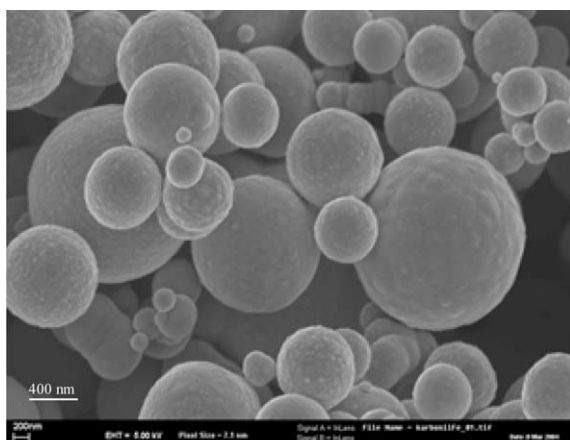
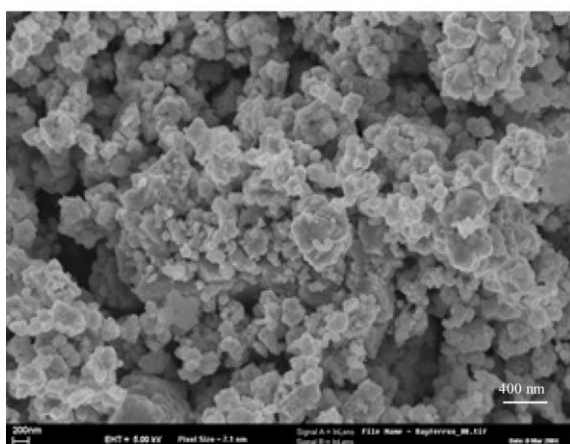


Fig. 2. Formation of bundles of magnetite particles in silicon oil, parallel to the field direction as seen by microscope. The concentration of magnetite in the mixture is 5 wt%. (a) No external magnetic field. (b) The magnetic induction 50 mT.



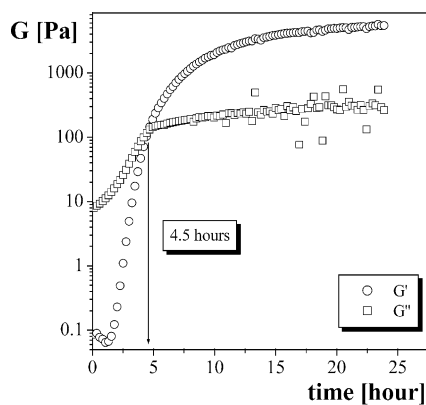
a



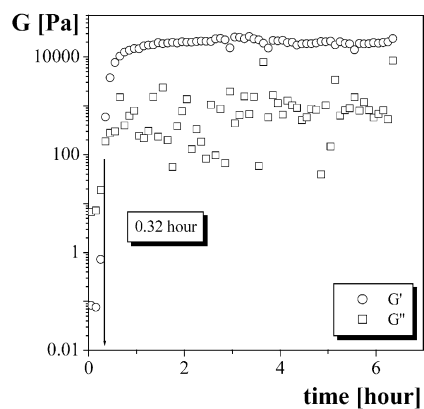
b

Fig. 3. SEM picture of the iron (a) and  $\text{Fe}_3\text{O}_4$  (b) particles. The bar corresponds to 400 nm.

diameter. According to the results of our preliminary frequency-sweep and strain-sweep experiments, 1 Hz and 5 Pa were used during the measurements. The results are shown on Fig. 4. This figure shows the change in the shear



a



b

Fig. 4. Determination of the gelling point at two different temperatures: (a) 25 °C, and (b) 60 °C.

storage modulus and the shear loss modulus in time. The gel point can be determined at the cross-over point of these curves. At 25 °C the gel point occurred at 4.5 h, while at 60 °C gelation took place after half an hour.

If the material is perfectly elastic then the stress wave is exactly in phase with the strain wave. For a purely viscous system when the rate of change of the sinusoidal oscillation is a maximum the strain is zero. Consequently the stress will be exactly 90° out-of-phase with the imposed deformation. In general the stress wave has a phase difference,  $\delta$  ( $0 < \delta < 90^\circ$ ), so that  $\delta$ , or more generally  $\text{tg}\delta$ , is a measure of the viscous/elastic ratio for the material at frequency  $\omega$ . The ratio of the out-of-phase shear loss modulus ( $G''$ ) to the in-phase shear storage modulus ( $G'$ ) determines the value of  $\text{tg}\delta$ :

$$\text{tg}\delta = \frac{G''}{G'} \quad (1)$$

To prepare a good elastomer, in other words to minimize the unreacted functionalities and pendant chains, the curing time must significantly exceed the gelling time. On the basis of these results the cross-linking reaction was carried out at ambient temperature for 4.5 h to obtain magnetoelasts.

After the gelation was completed, the cylindrical and cube shaped samples were removed from the mould and placed in silicone oil (DC 200 Fluka) in order to wash out the unreacted chemicals.

### 1.2.2. Poly(vinylalcohol) gels (PVA) with homogeneous filler distribution

Preparation of a magnetic poly(vinyl-alcohol) (MPVA) gel is similar to that of other filler-loaded elastomeric networks. One can precipitate well-dispersed particles in the polymeric material. The in situ precipitation can be made before, during and after the cross-linking reaction. First, a ferrofluid containing magnetite sol particles was prepared from  $\text{FeCl}_2$  and  $\text{FeCl}_3$  in aqueous solution. To counteract the van der Waals attraction and the attractive part of magnetic dipole interactions, colloidal stability was maintained by a small amount of  $\text{HClO}_4$ , which induced peptization. The

purified and stabilized magnetite sol having a concentration of 17.2 wt% was used for further preparative work [5–9]. Small angle X-ray scattering was used to determine the size and the size distribution of the magnetite particles in the sol. On Fig. 5 the result is shown. The average diameter of the particles is 4 nm and its distribution is fairly monodisperse.

For the preparation of the magnetic PVA gels 8 wt% PVA (Merck) solution and 1 M glutar-dialdehyde (Aldrich) were used as the polymer and the cross-linker, respectively. HCl was the initiator. The concentration of the magnetic particles in the gel was 1.2 wt%. The molar ratio between the monomer unit of polymer and the cross-linker was 300. After gelation the samples were kept in distilled water to remove the unreacted monomer.

### 1.2.3. Preparation of magnetoelasts with anisotropic mechanical behaviour

Synthesis of elastomers in a uniform magnetic field can be used to prepare anisotropic samples. Fig. 2(b) shows the pearl chain structuring of iron particles dispersed in silicon oil. The same phenomenon occurs if the silicon oil is replaced by the monomeric mixture of PDMS. If the polymerisation reaction does not proceed too fast, then there is enough time to induce the pearl chain structuring of the filler particles by applying a uniform external field. The chemical cross-linking locks in a chainlike particle structure aligned along the direction of the field. The resulting sample becomes highly anisotropic.

For the preparation the mixture of Elastosil 604 and magnetite particles was placed between the poles of a large electromagnet (JM-PE-I, JEOL, Japan) for 5 h at room temperature. The experimental setup is shown on Fig. 6. The uniform magnetic field was varied in a wide range from 10 to 400 mT. The formation of chain-like structure takes a few minutes and as a result, particle aggregates aligned parallel to the field direction are fixed in the network. Depending on the concentration of the magnetic particles as well as on the applied magnetic field, the columnar structures of the

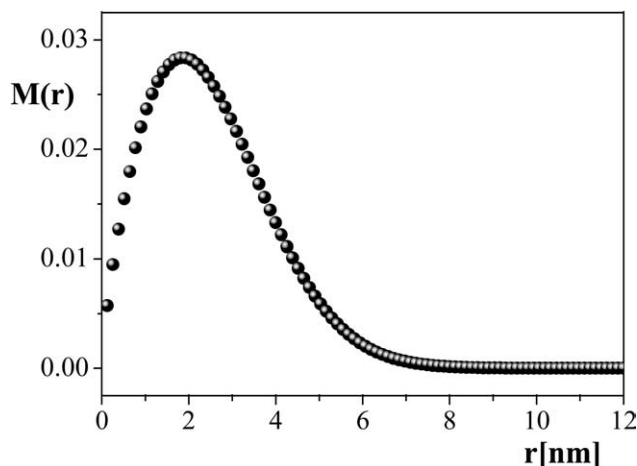


Fig. 5. The size distribution of the magnetite particles.

magnetic particles built into the elastic matrix can be varied in a wide range. One can easily vary the direction of the particle chains by the direction of the applied magnetic field as is illustrated on Fig. 6.

We have prepared several types of iron and  $\text{Fe}_3\text{O}_4$  loaded PDMS elastomers without external magnetic field and under a uniform magnetic field of 400 mT. During the preparation procedure the cross-linking density, as well as the concentration of filler particle were varied.

### 1.3. Mechanical measurements

We performed unidirectional stress–strain measurements to characterize the elastic properties of the magnetic composites. Static and dynamic mechanical tester (INSTRON 5543) was used for the experiment. Both large deformation as well as small deformation behaviour was investigated. In order to obtain the elastic modulus we have studied the small strain behaviour of magnetic composites. All the measurements were carried out at room temperature. The elastic modulus was determined by unidirectional compression measurements and the modulus,  $G$  was calculated on the basis of neo-Hookean law of rubber elasticity [19]:

$$\sigma_n = G(\lambda - \lambda^{-2}) = GD \quad (2)$$

where  $\sigma_n$  is the nominal stress defined as the ratio of the equilibrium elastic force and the undeformed cross-sectional area of the sample. The deformation ratio  $\lambda$  is the length,  $h$  (in the direction of the force) divided by the corresponding undeformed length,  $h_0$ .  $G$  stands for the modulus.  $D$  is equal to  $(\lambda - \lambda^{-2})$ . For non-ideal networks the Mooney–Rivlin representation is often used to characterize the stress–strain behaviour.

$$\frac{\sigma_n}{D} = C_1 + C_2\lambda^{-1} \quad (3)$$

where  $C_1 + C_2$  is identified as the modulus,  $G$ . The validity of Eq. (2) is supported by the mechanical measurements shown in Fig. 7, where Mooney–Rivlin plot is also presented.

The elastic modulus of the magnetic elastomers was determined on the basis of Eq. (2) from the plot of nominal stress against  $D$ . The slope, which provides the elastic modulus,  $G$  was calculated by linear least square method.

In case of filler loaded networks the elastic shear modulus ( $G$ ) can be expressed as a function of filler concentration by the Einstein–Smallwood equation [10]:

$$G = G_0(1 + k_e\phi_m) \quad (4)$$

where  $G_0$  denotes the modulus of the elastomer without solid particles,  $k_e$  is the Einstein–Smallwood parameter and  $\phi_m$  represents the volume fraction of the filler particles. For non-interacting spherical particles  $k_e = 2.5$  is predicted.

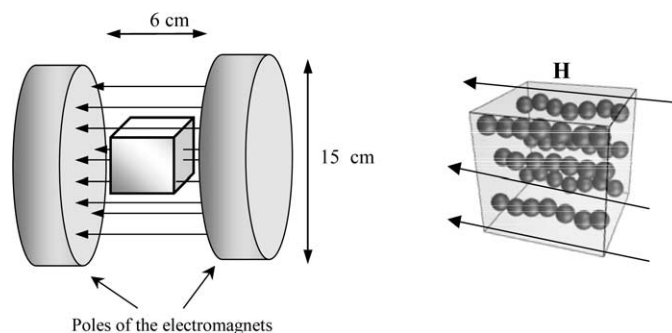


Fig. 6. Preparation of uniaxially ordered polymer composite under uniform magnetic field.

## 2. Results and discussion

### 2.1. Anisotropic behaviour as seen by the naked eye

The anisotropy manifests itself both in direction dependent elastic modulus as well as direction dependent swelling. Fig. 8 shows a magnetite-loaded PDMS elastomer in three different states. The magnetite content of the magnetoelast is 40 wt%. At the left of figure (a) the sample is stress-free. The arrow indicates the direction of the chain-like particle orientation. On the middle, a load of 50 g is placed on the top of the sample.

The anisotropy also manifests itself during swelling. Fig. 8(b) and (c) shows the effect of swelling on the same  $\text{Fe}_3\text{O}_4$  loaded magnetoelast as a swelling agent, *n*-hexane, was used at room temperature. Since, the swelling degree and elastic modulus are interrelated, the swollen gel shows anisotropy. The swelling degree parallel to the chain-like particle orientation is less in perpendicular direction.

### 2.2. Results of mechanical measurements at small deformation

Results of stress–strain measurements for isotropic PDMS magnetoelasts are shown in Fig. 7. This figure clearly indicates that within the experimental accuracy the unidirectional stress–strain behavior of magnetic PDMS elastomers having different amount of iron particles dispersed randomly into the polymer matrix obeys the neo-Hookean law. Deviation from the ideal behavior, characterized by the second Mooney–Rivlin constant,  $C_2$  can be neglected.

This is not the case for anisotropic samples. There are two different situations when comparing the direction of mechanical stress to the particles alignment. The direction of the compression can either be perpendicular or parallel to the pearl chain structure locked into the PDMS network. When the direction of the compressive force is perpendicular to the pearl chain structure, we have found a slight deviation from the ideal behaviour as shown in Fig. 9.

It was found that in many cases a non-ideal mechanical behaviour occur with a slight negative  $C_2$ .

The deviation from the ideal behaviour is much more

significant if the direction of the compressive force is parallel to the chain-like structure. This is demonstrated in Fig. 10. The second Mooney–Rivlin constant was found to be always negative  $C_2 < 0$ .

We have also checked the validity of Eq. (4). It was found that Einstein–Smallwood parameter  $k_e = 3.36 \pm 0.49$  for the isotropic sample. This value is close to the theoretical value of 2.5. For anisotropic sample when the compression is perpendicular to the chain formation,  $k_e$  was found to be  $2.82 \pm 0.22$ . A very large deviation has been found when the compression is parallel to the chain formation. In this case  $k_e = 40.02 \pm 8.19$  was obtained. The large deviation can be explained by the strong mutual particle–particle interaction, because the theoretical value of Einstein–Smallwood parameter is valid for the spherical shaped, non-interacted systems.

On the basis of the Einstein–Smallwood equation (Eq. (2)) one expects that the reinforcement is due to the concentration of filler particles. We have found that not only the particle concentration, but also the spatial distribution of the solid particles influences the mechanical behaviour.

Fig. 11 shows the strong influence of the particle arrangement on the elastic modulus at different iron contents. The iron content was varied from 10 to 30 wt%. The component B content was 2.5 wt%.

This figure shows that the pearl chain structure of the particles in the polymer matrix results in strongly anisotropic mechanical behaviour. The modulus increases substantially if the direction of the particle chains is parallel to the particle alignment. The smallest modulus is obtained when the mechanical stress is perpendicular to the direction of the particle chains. The elastic modulus of the sample increased with increasing the iron content. In the case of the isotropic sample and when the direction of the deformation is perpendicular to the pearl chain structure, the increment in the elastic modulus were within 5% experimental error and the columnar structure of the particles did not affect the modulus. However, the elastic modulus increased drastically with the iron content, as the direction of the compression was parallel to the pearl chain structure. At 30 wt% iron content the modulus increased by 250%.

To characterize the effect of cross-linking density, the content of Elastosil 604 B component varied from 2.45 to

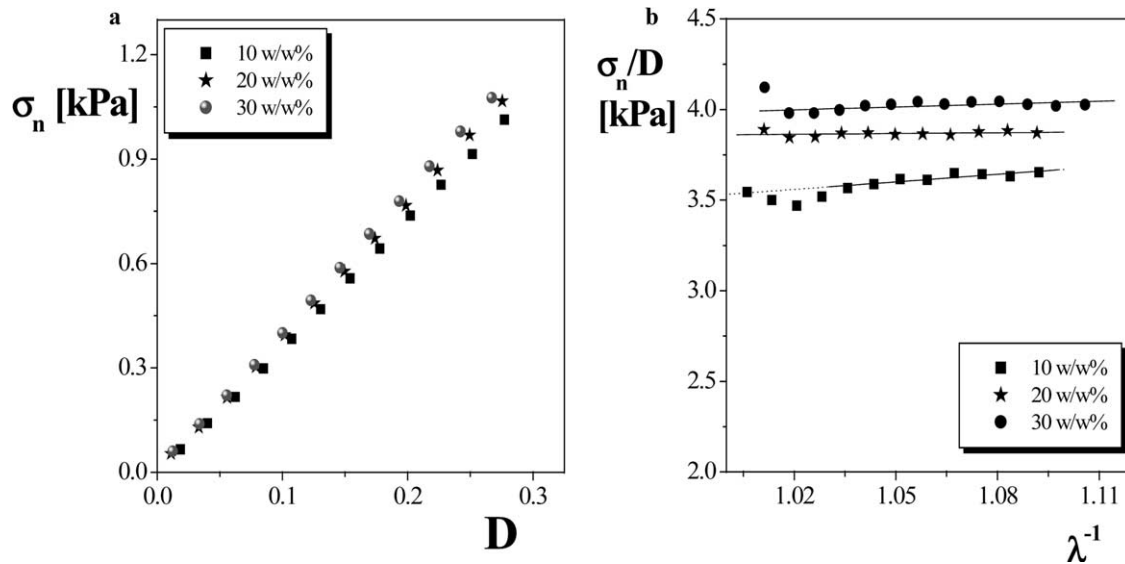


Fig. 7. Stress–strain measurements for PDMS samples filled with randomly distributed carbonyl iron particles. Symbols represent different amount of iron particles indicated in the figure.

3.48 wt%. In these experiments the concentration of the iron was 30 wt%. The dependence of the elastic modulus on the amount of component B is shown in Fig. 12.

Fig. 12 shows the effect of cross-linking density on the elastic modulus. It also emphasises that the spatial distribution of magnetic particles makes its influence felt on the modulus. Increasing the cross-linking density, the elastic modulus increases. However, the increment is more pronounced when the direction of the deformation is parallel to the particle alignment. The weakest effect characterizes the perpendicular case.

### 2.2.1. Anisotropic magnetic PVA gel and iron loaded PDMS networks at large deformation

Unidirectional compression measurements were performed on the anisotropic magnetic PVA and PDMS samples. Stress–strain dependence for magnetic PVA gels as well as for magnetic PDMS samples with random and aligned structure is shown in Fig. 13. When comparing the shape of the curves one can find significant differences. Not only the slope (elastic modulus,  $G$ ) depends on the filler structure locked in the elastic materials, but also the shape of the curves is different. The field structured composite along the chainlike structure exhibit significantly larger modulus. One can also see a characteristic change in the slope of the stress–strain curve of the anisotropic samples when the direction of the compression is parallel to the pearl chain structure.

The stress–strain curve for magnetic PVA gel filled with magnetite shows a bending point (Fig. 13(a)) if the compression and particle alignment are parallel. The critical strain at which the bending occurs was found to be  $\lambda_c = 0.85$ . At larger deformation  $\lambda < \lambda_c$  the slope (elastic modulus) decreases, which means a stress induced softening

phenomenon. The softening may be interpreted as a mechanical instability due to the presence of rod-like particle chains. The behaviour of a rod subjected to longitudinal compressing force was first investigated by Euler. It was found that at small compressing force the rods are stable with respect to any small perturbations. This means that the rods are slightly bent by some compressive force and it will tend to return to its original shape when the force ceases to act. If the compressive force exceeds a critical value,  $f_c$  a mechanical instability occurs. This results in a large bending. The behaviour of bending above the critical strain,  $\lambda_c$  requires less force ( $f < f_c$ ) for the further deformation. The softening phenomenon is shown in Fig. 14.

When the deformation ratio reaches the value 0.9 the pearl chain structure started to bend under the compression, because the polymer chains in the PVA network interact with the magnetic particle as shown in Fig. 14. The ordered structure of the particles and the interaction with the polymer network prevent the pearl chain structure of the particles from being destroyed by compression. The parallel deformation to the structure has a strong influence on the mechanical behaviour because of the bending of the ordered structure. The anisotropic  $\text{Fe}_3\text{O}_4$  loaded PDMS samples showed the similar behaviour under compression.

In contrast to the magnetic PVA gels, the compression of the iron loaded PDMS network results in a break point in the stress–strain curve if the deformation of the sample is parallel to the pearl chain structure. Fig. 13(b) shows that the nominal stress increases with the compression up to a deformation ratio of 0.95 in every case. On increasing the compression above this ratio the columnar structures of the iron particle are destroyed as Fig. 15 shows.

In a uniform magnetic field the iron particles interact

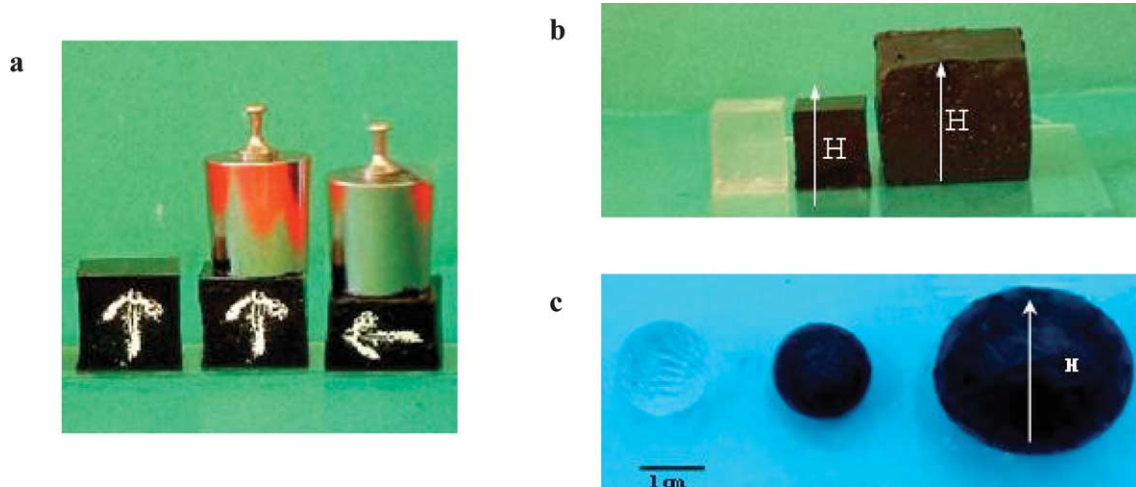


Fig. 8. Anisotropic mechanical (a) and swelling (b) and (c) behaviour as seen by the naked eye. The arrow indicates the direction of the magnetic field during the preparation.

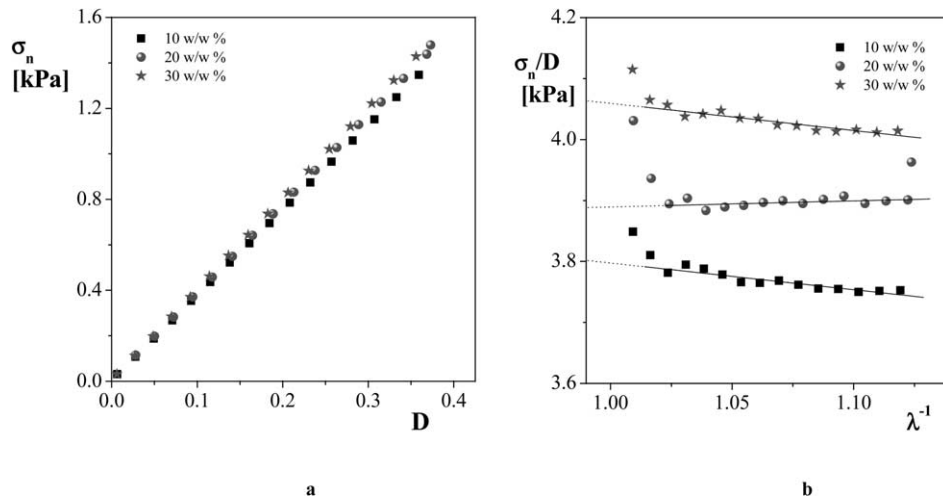


Fig. 9. Unidirectional compression data for anisotropic PDMS samples filled with carbonyl-iron. The compression is perpendicular to the direction of pearl chain-like structure locked in the elastomer. Symbols represent different amount of iron particles.

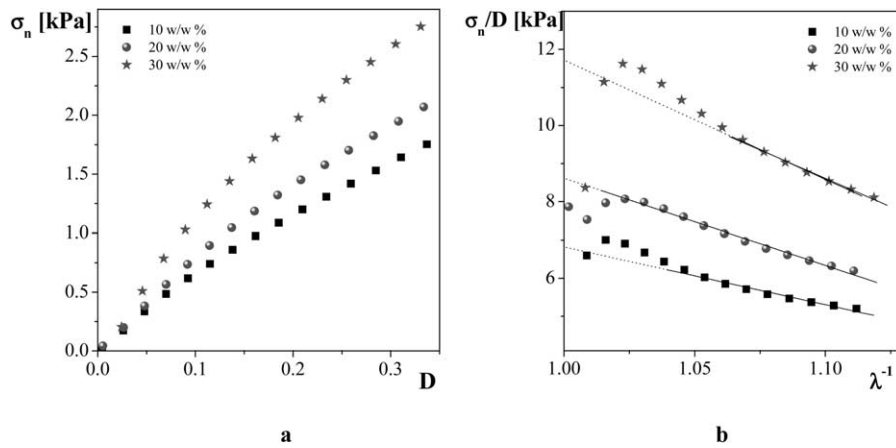


Fig. 10. Unidirectional compression data for anisotropic PDMS samples filled with carbonyl-iron. The compression is parallel to the direction of chain-like structure. Symbols represent different amount of iron particles indicated on the figure.

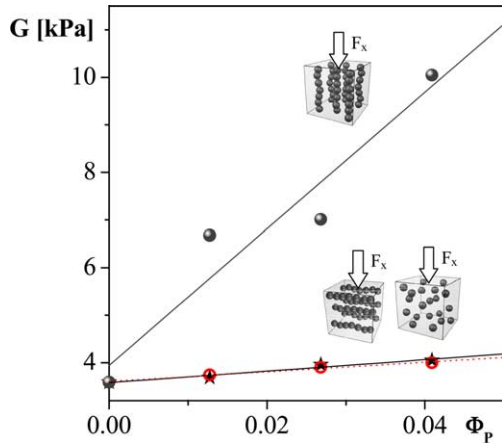


Fig. 11. The influence of the iron content and the particle arrangement on the elastic modulus.  $F_x$  shows the direction of deformation.

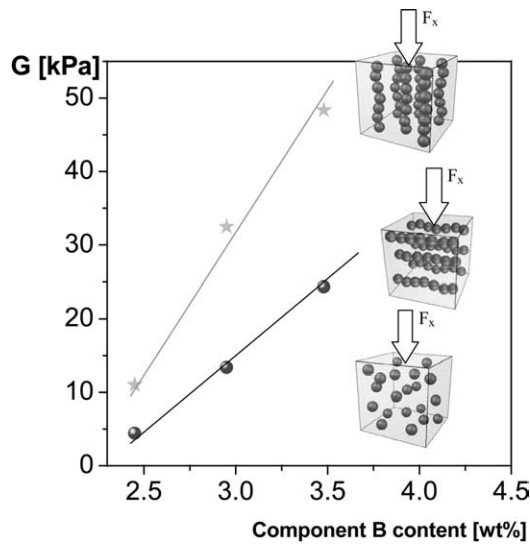


Fig. 12. The influence of the cross-linking density and the particle arrangement on the elastic modulus.  $F_x$  shows the direction of deformation.

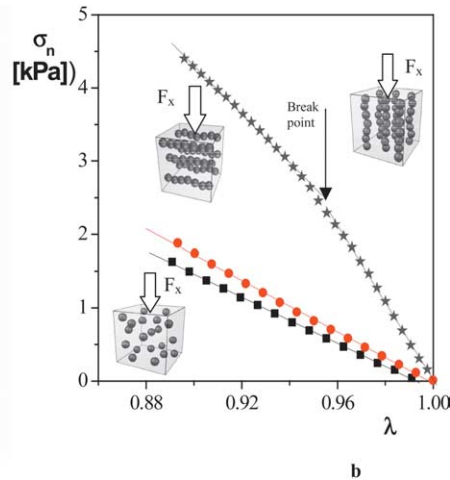
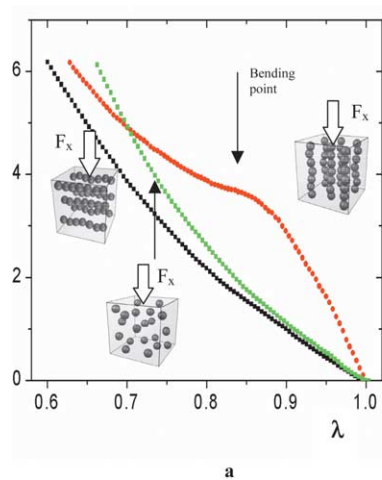


Fig. 13. Typical stress–strain behaviour of magnetic PVA gels and PDMS elastomers in unidirectional compression measurements. (a) Magnetic PVA gel. (b) Iron loaded PDMS elastomers. In both cases three samples are compared having the same amount of filler particles, but the distribution of the particles is different as indicated in the figure.

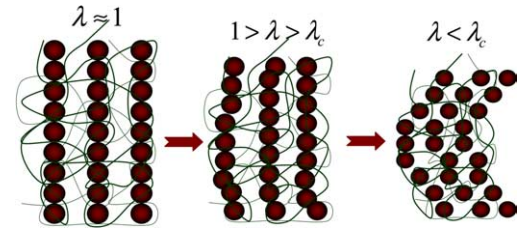


Fig. 14. Schematic picture of the bending of the magnetic PVA gels under compression.

with each other, but the particles do not interact with the polymer network. The polymer network can immobilise the ordered structure, but it cannot prevent the break-up of the ordered structure under compression. The iron particles in the chains slip out from the columnar structure under compression, breaking the ordered structure as shown schematically in Fig. 15.

In order to characterize the bending or breaking phenomena we have defined an apparent elastic modulus ( $G_a$ ) as follows:

$$G_a = \frac{\partial \sigma_n}{\partial D} \tag{5}$$

Fig. 16 shows the dependence of the apparent elastic modulus on the quantity  $D$ . For the sake of comparison

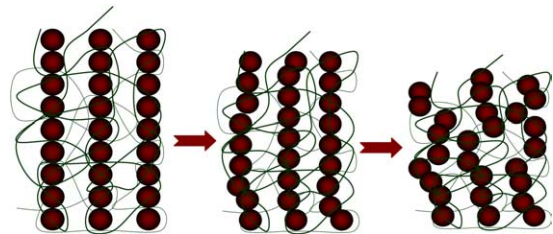


Fig. 15. Structural change of the iron loaded PDMS elastomer under compression.



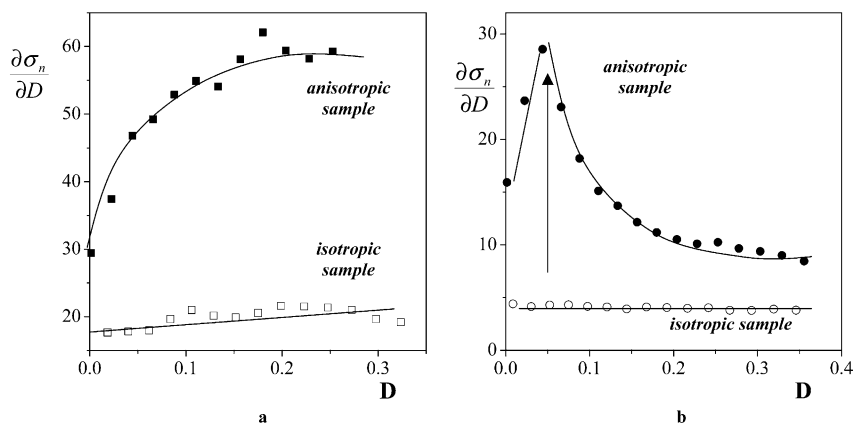


Fig. 16. Change in the apparent elastic modulus due to compression: (a)  $\text{Fe}_3\text{O}_4$  loaded PDMS sample, (b) iron loaded PDMS sample. Solid lines are guides for eyes, the arrow indicate the breaking point.

results of compression measurements performed on both isotropic and non-isotropic samples are shown. The composites contain  $\text{Fe}_3\text{O}_4$  filler particles with concentration of 30 wt%. In case of isotropic sample the apparent elastic modulus increases slightly within the experimental error of 5%. For anisotropic sample the apparent modulus increases significantly under deformation up to the value  $D=0.85$ . Above this value the modulus does not change notably.

Fig. 16(b) shows the results of PDMS composites filled with carbonyl iron. The concentration of filler particles is 30 wt%. One can see the breaking of the pearl chain structure at  $\lambda=0.95$ .

It is also seen that the change of the apparent elastic modulus of the isotropic sample is negligible. For the anisotropic samples the apparent elastic modulus increases significantly under deformation up to the value 0.05  $D$ . Above this value the modulus decreases notably, which can be explained by the broken structure.

### 3. Summary of the main results

We have demonstrated that the interactions in colloidal particles can be easily tuned by external magnetic field and the chemical process can fix the structured lane formation. The result is a highly anisotropic sample. We have shown that uniaxial field structured composites consisting of magnetic particles in the elastomer exhibit a larger increase in modulus than random particle dispersions. According to the measurements the increase in the elastic modulus is most significant if the applied stress is parallel to the particle alignment. The anisotropy manifests itself both in a directionally dependent elastic modulus as well as in directionally dependent swelling. Since, the physical properties such as elastic modulus, stress-strain behaviour and swelling along- and perpendicular of the chain-like structure are significantly different, therefore, these materials may find usage in elastomer bearings and vibration absorber. Anisotropic magnetic elastomers are worth further experimental and theoretical study.

### Acknowledgements

This research was supported by the Széchenyi NRDP No. 3/043/2001 and the Hungarian National Research Fund (OTKA, Grant No. T038228 and F046461). This research is sponsored by NATO's Scientific Division in the framework of the Science for Peace Programme.

### References

- [1] Zrínyi M, Barsi L, Büki A. *J Chem Phys* 1996;104(20):8750–6.
- [2] Zrínyi M, Barsi L, Büki A. *Polym Gels Networks* 1997;5:415–27.
- [3] Szabó D, Barsi L, Büki A, Zrínyi M. *Models Chem* 1997;134(2/3): 155–67.
- [4] Zrínyi M. *Trends Polym Sci* 1997;5(9):280–5.
- [5] Zrínyi M, Barsi L, Szabó D, Kilian HG. *J Chem Phys* 1997;108(13): 5685–92.
- [6] Bernadec S. *J Magn Magn Mater* 1997;166:91–6.
- [7] Martin JE, Anderson RA. *J Chem Phys* 1999;111(9):4273–80.
- [8] Zrínyi M, Szabó D, Barsi L. Magnetic field sensitive polymeric actuators. In: Osada Y, Rossi DE, editors. *Polymer sensors and actuators*. Berlin: Springer; 1999. p. 385–408.
- [9] Bernadec S. *Appl Phys A* 1999;68:63–7.
- [10] Carlson JD, Jolly MR. *Mechatronics* 2000;10:555–69.
- [11] Borcea L, Bruno O. *J Mech Phys Solids* 2001;49:2877–919.
- [12] Ginder JM, Clark SM, Schlotter WF, Nichols ME. *Int J Mod Phys B* 2002;16(17/18):2412–8.
- [13] Zrínyi M, Szabó D, Filipcsei G, Fehér J. Electric and magnetic field sensitive smart polymer gels and networks. Osada/Khokhlov, editors. New York: Marcel Dekker; 2002. p. 309–55 [Chapter 11].
- [14] Mitsumata T, Furukawa K, Juliac E, Iwakura K, Koyama K. *Int J Mod Phys B* 2002;16(17/18):2419–25.
- [15] Rosenweig E. *Ferrohydrodynamics*. Cambridge: Cambridge University Press; 1985.
- [16] Raikher YuL, Stolbov OV. *J Magn Magn Mater* 2003;(258/259): 477–9.
- [17] Zhou GY, Jiang ZY. *Smart Mater Struct* 2004;13:309–16.
- [18] Berkovski B, Bashtovoy V, editors. *Magnetic fluids and applications handbook*. New York: Begell House; 1996.
- [19] Landau LD, Lifshitz EM. *Theory of elasticity*. New York: Pergamon Press; 1989.